



Improvement of biohydrogen generation and seawater desalination in a microbial electro dialysis cell by installing the direct proton transfer pathway between the anode and cathode chambers

Euntae Yang^a, Mi-Jin Choi^b, Kyoung-Yeol Kim^a, In S. Kim^{a,*}

^a*School of Environmental Science and Engineering, Gwangju Institute of Science and Technology (GIST), 261 Cheomdan-gwagiro, Gwangju, Buk-gu 500-712, South Korea*

Tel. +82 62 715 3381; Fax: +82 62 715 2584; email: iskim@gist.ac.kr

^b*Department of Electrical and Computer Engineering, Texas A&M University, College Station, TX 77843-3128, USA*

ABSTRACT

We are focusing on the enhancement of microbial electro dialysis cell (MEDC) performance by alleviation of pH gradient between the anode and cathode chambers by setting up a direct proton transfer pathway, which allows protons to migration unconstrainedly, with three different membranes ultrafiltration membrane (UF), anion-exchange membrane (AEM), cation-exchange membrane (CEM)) in the MEDC. Setting up a direct proton transfer pathway between the anode and cathode chamber in the MEDC abated pH gradient by up to about 54%. Also, hydrogen production and salt removal efficiency were enhanced. In a comparison of membranes for a direct proton transfer pathway, an AEM has the best performance for reduction for pH gradient because of a higher proton transfer by phosphate anions, but due to the high substrate permeability of an AEM, the hydrogen production with AEM was lower than that with UF—which highest hydrogen production was observed with UF (5.77 ± 0.54 mL, 0.55 ± 0.14 mL/h). In terms of salt removal efficiency, using CEM as a direct proton transfer pathway showed the highest performance (77.63%)

Keywords: Desalination; Direct proton transfer pathway; Hydrogen; Microbial electro dialysis cell; pH gradient

1. Introduction

Fossil fuels are primary energy source of modern civilization. However, the excessive dependence on fossil fuels leads to serious environmental problems and human health problems [1]. Thus, hydrogen is spotlighted as the upcoming alternative energy source

because of its environmental friendliness (free from carbon dioxide). However, contemporarily, 95% of world hydrogen gas is generated from fossil fuels, principally, by the way of the steam reforming natural gas, causing the unrestrained emission of carbon dioxide, which contribute to climate change [2]; thus, environmental friendly hydrogen gas production methods are strongly required [3].

Biological hydrogen production technologies, such as direct bio-photolysis, indirect bio-photolysis, photo

*Corresponding author.

fermentation, dark fermentation, and bioelectrochemical system (BES), have gained great attentions, because these biological technologies utilize waste biomass, and these biological processes are generally run at room temperature and atmospheric pressure [4–6]. In particular, BES, which produces hydrogen by the combination of the anodic bacterial oxidation and the cathodic reduction reaction with the assistance of external power source, is regarded as a promising biohydrogen production technology, because BES has shown more effective and practicable hydrogen production [5,7].

Recently, to BES, the function of seawater desalination has been added by inserting a middle chamber for desalination between the anode and cathode chambers. This modified BES is referred to as microbial electrodiolysis cell (MEDC). The MEDC can simultaneously produce hydrogen and desalinate seawater by the following mechanisms: The electrons are generated through organic matter oxidation by electrochemically active bacteria (EAB) in the anode chamber, and then move into the cathode chamber for hydrogen production by the assistance of external power source. At the same time, to maintain charge balance, in the middle chamber chloride ions transfer to the anode chamber through an anion-exchange membrane (AEM), and sodium ions migrate into the cathode chamber through a cation-exchange membrane (CEM) [8].

This MEDC has several crucial benefits compared with other hydrogen production technologies and desalination technologies. Firstly, MEDC can perform the hydrogen evolution and seawater desalination with much lower energy consumption (0.4–0.8 V) compared with a water electrolysis (1.8 V) for hydrogen production, and reverse osmosis (RO, 3–8 kWh/m³) and thermal desalination technologies (10–25 kWh/m³) for seawater desalination [9,10]. Secondly, the pure hydrogen gas (100%) was generated in the cathode chamber in MEDC compared with other anaerobic digestion processes [11].

However, MEDC is faced with several common drawbacks. The most common is a pH gradient between the anode and cathode chamber, since the protons generated by the bacterial oxidation accumulate in the anode chamber due to the AEM prohibiting proton transfer. In the consequence of inhibiting the proton transfer, in the cathode, protons for the hydrogen production was provided from the catholyte buffer solution so that the proton was consumed more than the buffer capacity. Therefore, the pH value of both chambers was significantly changed with the anolyte pH decreases and the catholyte pH increases. This pH gradient leads to a decrease in the viability of EAB and increase in potential loss in MEDC.

In order to alleviate the imbalance of pH between the anode and cathode chambers, the direct pathway of proton transfer between the anode and cathode chamber was set up in a cubic-shaped MEDC reactor. The direct proton transfer pathway enables protons to migrate freely from the anode chamber to the cathode chamber by directly connecting both two chambers. To access the effect of the direct proton transfer pathway, the performance of MEDC with the direct proton transfer pathway constructed with different types of membranes (AEM, CEM, and ultra-filtration membrane (UF)) was evaluated and compared with that of the conventional MEDC in terms of hydrogen production rate, pH variation in each chamber, and the salt removal rate in the desalination chamber.

2. Materials and methods

2.1. MEDC setup

As shown in Fig. 1, a three chambered MEDC based on a cubic-shaped MFC was set up. The MEDC consisted of an anode chamber (200 mL volume), a cathode chamber (200 mL volume), and a middle chamber (50 mL volume). In order to install direct pathway for proton transfer between the anode chamber and cathode chamber in the MEDC, the desalination chamber was horizontally divided into two compartments by using acrylic bar (Fig. 2). The upper compartment of the middle chamber was operated at desalination, and the bottom compartment was employed as the direct proton transfer pathway from the anode chamber to the cathode chamber. The AEM (AMX, Neosepta, Japan) was used to separate the anode chamber and the upper compartment, and the CEM (Nafion 117, Dupont, USA) was used to separate the upper compartment and the cathode chamber. In the direct proton transfer pathway, different type of separators (Ultrafiltration membrane (UF, MWCO 1 kDa, Millipore, USA), AEM (AMX, Neosepta, Japan), CEM (Nafion 117, Dupont, USA)) was set up. Carbon felt (25 cm², 6 mm thickness, Morgan, UK) glued onto a perforated stainless steel plate with conductive silver paste was used as a anodic electrode, and a perforated stainless steel plate (working area 25 cm²)-coated platinum (0.5 mg/cm²) was used as a cathodic electrode. The headspace of the cathode chamber was maintained at 300 cm³.

2.2. Medium

Nutrient mineral buffer solution (NMB, pH 7), used as the anolyte, contained 6.0 g/L NaH₂SO₄,

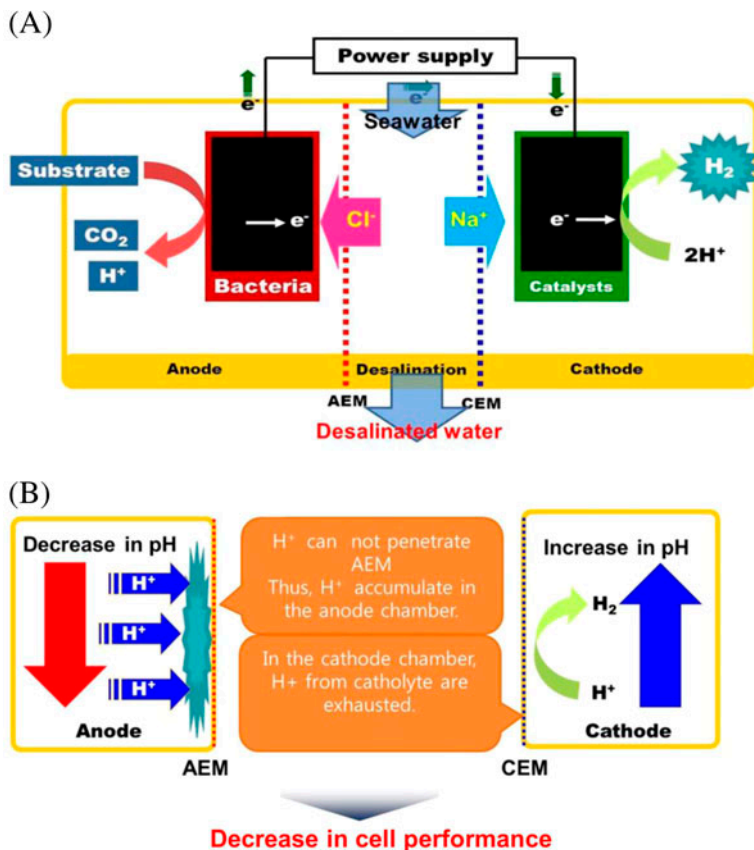


Fig. 1. (A) The schematic diagram of a cubic-shaped three chambered MEDC and (B) the mechanism of pH-gradient between the anode and cathode chambers in an MEDC.

530 mg/L NH_4Cl , 200 mg/L $\text{MgCl}_2 \cdot \text{H}_2\text{O}$, 150 mg/L CaCl_2 , 2.5 mg/L $\text{CoCl}_2 \cdot 6\text{H}_2\text{O}$, 0.05 mg/L $\text{NaMoO}_4 \cdot 2\text{H}_2\text{O}$, 20 mg/L $\text{FeCl}_2 \cdot 4\text{H}_2\text{O}$, 0.25 mg/L $\text{NiCl}_2 \cdot 4\text{H}_2\text{O}$, 0.5 mg/L $\text{MnCl}_2 \cdot 4\text{H}_2\text{O}$, 0.25 mg/L Na_2SeO_4 , 0.05 mg/L $\text{NaVO}_3 \cdot 4\text{H}_2\text{O}$, 0.25 mg/L ZnCl_2 , and 0.15 mg/L CuCl_2 [12]. The catholyte used was phosphate buffer solution (PBS, 50 mM, pH 7). The water to be desalinated was artificial seawater, at NaCl concentration of 5, 20, 35 g/L.

2.3. Operating conditions

The anode was inoculated with anaerobic digester sludge (20% v/v) from Gwangju sewage treatment plant in South Korea. Before operating MEDC, the anode was acclimated to acetate in the conventional microbial fuel cell (MFC) at a 600Ω of resistance for 6 months. In order to conduct the experiment with MEDC, the MFC reactor was shifted to MEDC reactor. The anode chamber, the cathode chamber, and the desalination chamber were filled with 150 mL of NMB, 165 mL of PBS, and 20 mL of artificial seawater each. Dissolved oxygen was removed from the anode and cathode chambers using pure nitrogen gas over

15 min. Acetate was utilized as a sole substrate. A voltage of 500 mV was applied to the MEDC reactor by a power supply (N6700B, Agilent Technologies, USA). A single batch cycle was regarded complete when the anode potential attained -10 mV. The experiments were divided into two parts. The experiments in the first part were carried out with the conventional MEDC, which do not have the direct proton transfer pathway. Then, the experiments in the second part were performed with the modified MEDC having the direct proton transfer pathway with different separators (MEDC–AEM, MEDC–CEM, MEDC–UF). Each experiment was performed triplicate in a temperature controlled room at 25°C .

2.4. Analyses and calculations

The potential of the anode and cathode electrodes were continuously monitored using a multimeter (2,700 Data acquisition series, Keithley, USA) versus Ag/AgCl reference electrode (Microelectrode Inc, USA), inserted in each chamber. The current was determined by measuring voltage across a 5Ω of

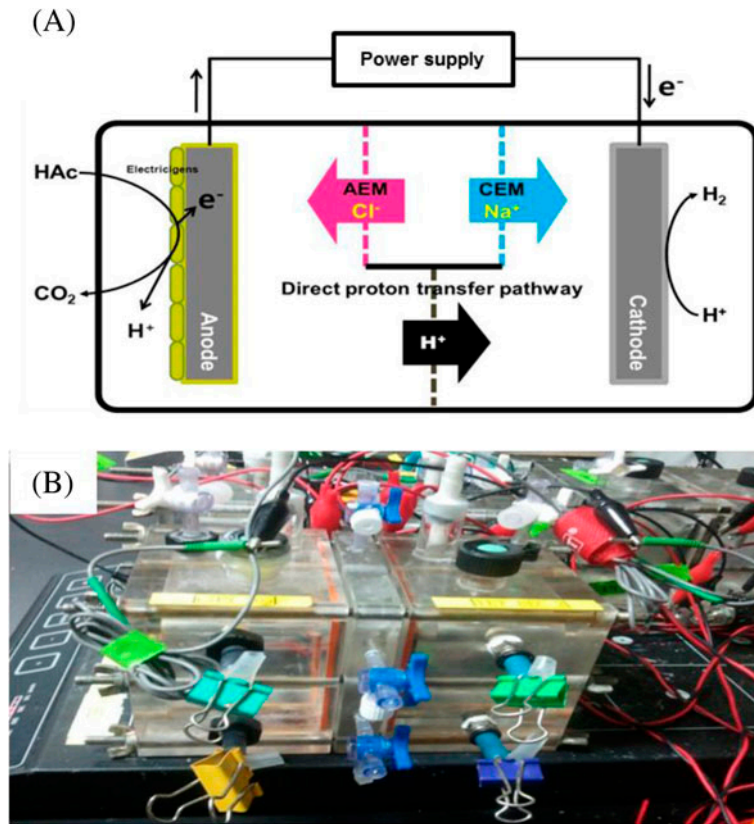


Fig. 2. The cubic-shaped three chambered MEDC with direct proton transfer pathway (A) schematic and (B) photograph.

external resistance. At the beginning and end of each batch cycle, total dissolved solids (TDS) and pH were measured using a TDS meter (EC-40N, iSTEK, Korea) and a pH meter (Orion 3 star, Thermo Scientific, USA)

The gas production was analyzed by using a gas chromatography (GC 2010, Shimadzu, Japan) with a thermal conductivity detector (TCD), capillary column (CP-Pora PLOT Q 27.5 m × 0.53 m, 20 μm) and ultra-high purity nitrogen gas (99.999%) as a carrier gas.

To evaluate the performance of the MEDCs, salt removal rate, the hydrogen production rate, anodic conversion efficiency, cathodic conversion efficiency, and overall hydrogen conversion efficiency were calculated.

The desalination rate and efficiency was determined based on the measurement of TDS at the start and end of a single-batch cycle.

The hydrogen production rate (Q) was determined by Eq. (1),

$$Q = \frac{V_{\max H_2}}{T} \quad (1)$$

where $V_{\max H_2}$ (mL) is the maximum volumetric hydrogen production for each batch cycle, T is time period

of maximum volumetric hydrogen production for each batch cycle.

The anodic conversion efficiency (ACE) is calculated by Eq. (2),

$$ACE = \frac{C_p}{C_T} \times 100 (\%) \quad (2)$$

where C_p is the Coulombs calculated by integrating the measured current over time, C_T is the theoretical number of Coulombs produced from substrate. C_T can be calculated by Eq. (3),

$$C_T = \frac{FbSv}{M} \quad (3)$$

where F is Faraday's constant (96,485 C/mol electrons), b is the number of moles of electrons produced per mole of substrate (eight electrons from acetate), S is the concentration of the substrate, v is the volume of liquid, and M is the molecular weight of the substrate (82 g/mol).

The cathodic conversion efficiency (CCE) is calculated as

$$CCE = \frac{n_{H_2}}{C_p} \quad (4)$$

where n_{H_2} is the number of moles of hydrogen generated during a batch cycle. The overall hydrogen conversion efficiency (OE) is determined by the ratio of the actual total number of Coulombs converted to hydrogen in the cathode to the theoretical number of coulombs.

3. Results and discussion

3.1. pH changes in the anode and cathode chambers

During the operation of a conventional MEDC, severe pH gradients between the anode and cathode chambers, which worsen the performance of MEDC, occurs due to the limitation of proton transfer between the anode and cathode chambers by an AEM [13]; thus, a direct proton transfer pathway was installed in MEDCs to prevent pH in the anode and cathode chambers from changing. In order to evaluate the effect of the installation of a direct proton transfer pathway between the anode and cathode chambers in a MEDC, the conventional MEDC and the MEDCs with a direct proton transfer pathway constructed with different types of membranes, such as UF, AEM, and CEM, were operated in a batch mode.

Fig. 3 provides results for the pH changes in the anode and cathode chambers of each MEDC. The initial pH of the anode and cathode chambers in all the experiments was 7.0. As expected, the highest pH variations in the anode and cathode chambers were observed during the operation of the conventional MEDC (0.45 pH drop in the anode chamber, and 0.29 pH increase in the cathode chamber), followed by the MEDC–CEM (0.33 pH drop in the anode chamber, 0.16 pH increase in the cathode chamber), the MEDC–UF

(0.31 pH drop in the anode chamber, 0.14 pH increase in the cathode chamber), and the MEDC–AEM (0.27 pH drop in the anode chamber, 0.06 pH increase in the cathode chamber). These results clearly show that a direct proton transfer pathway can reduce the pH gradients between the anode and cathode chambers in MEDCs by allowing protons, released by the EAB, to move from the anode chamber to the cathode chamber.

However, the ability of a direct proton transfer pathway to soften pH gradients varies according to the types of membrane, used for a direct proton transfer pathway. The higher pH variations were demonstrated during the operation of the MEDC–CEM than that of the MEDC–AEM and the MEDC–UF; In BESs, a CEM shows the poor proton transfer ability because the CEM is preoccupied by other mono- and divalence cations, such as Na^+ and Ca^{2+} , for bacterial growth: generally, other cations exist at 10^5 times higher than protons do in the electrolyte for the operation of BESs [14]. In contrast, the MEDC–AEM showed lower pH variations than the MEDC–CEM. When using an AEM with phosphate buffer in BES, the imbalance of pH can be reduced compared with when using a CEM in BES because an AEM allows phosphate anions to play a rule as proton carrier as well as a buffer [15]. Also, the MEDC–UF showed the lower pH variation in the MEDC–CEM because protons can efficiently migrate from anode to cathode through the pores of the UF [16].

3.2. Hydrogen production

Fig. 4 describes the maximum hydrogen productions and hydrogen production rates during the

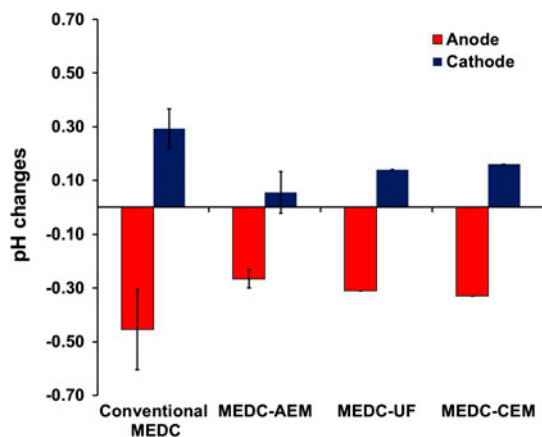


Fig. 3. pH variations in the anode and cathode chambers in the MEDCs. The initial pH of the anode and cathode chambers was pH 7.

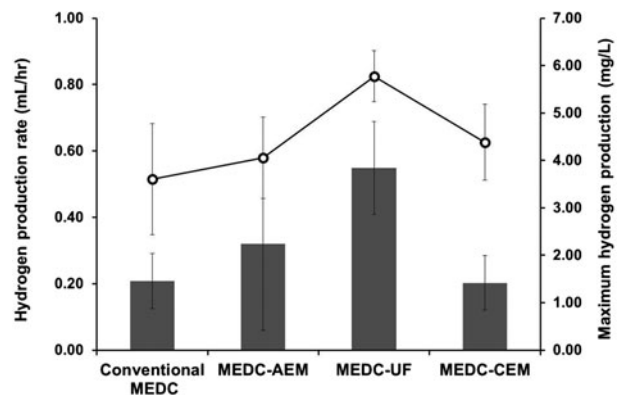


Fig. 4. The hydrogen production rate and the amount of hydrogen production during operating the conventional MEDC and MEDCs with a direct proton transfer pathway constructed with three different types of membranes.

Table 1
Coulombic efficiency, cathodic conversion efficiency, and overall hydrogen conversion efficiency

Direct proton transfer pathway	ACE (%)	CCE (%)	OE (%)
Conventional MEDC	78.15	38.36	30.37
MEDC–AEM	84.67	35.82	27.37
MEDC–UF	87.74	32.17	32.21
MEDC–CEM	88.65	22.53	19.97

operation of the conventional MEDC and MEDCs with a direct proton pathway constructed with three different membranes. Note that the MEDCs having a direct proton pathway showed relatively higher maximum hydrogen production and hydrogen production rate than the conventional MEDC did. These results indicate that the installation of a direct proton transfer pathway could positively affect hydrogen production in the MEDC system.

Also, a clear difference in hydrogen production was observed as a type of membrane used for a direct proton transfer pathway. The greatest maximum hydrogen production (5.77 ± 0.54 mL) and hydrogen production rate (0.55 ± 0.14 mL/h) were obtained the MEDC–UF because of a high proton transfer ability of UF. Even though MEDC–AEM showed the most outstanding ability to reduce pH variations, the maximum hydrogen production (4.06 ± 0.54 mL) and hydrogen production rate (0.32 ± 0.26 mL/h) was much lower than MEDC–UF. It may be due to substrate losses from the anode chamber caused by the substrate permeating the AEM [17]. In addition, an AEM is prone to bend away from the cathode. As a result of this deformation, a void space of water is created; therefore the internal resistance of the MEDC system would be increased [18].

3.3. Conversion efficiencies

Table 1 illustrates conversion efficiencies in each chamber (ACE, CCE) and OE for the conventional MEDC and MEDCs with a direct electron transfer pathway constructed with different types of membranes. The conventional MEDC showed much lower ACE compared with the MEDCs with a direct transfer pathway (78.15%); because pH decrease in the anode chamber would inhibit the viability of EAB.

In contrast to ACE, the higher CCE was observed in a conventional MEDC (38.36%) than that in MEDCs with a direct proton transfer pathway. In this study, it could not be found the exact correlation between an installation of direct proton transfer pathway and

CCE in MEDC systems, but the possible reasons for the lowest CCE observed in the MEDC–CEM are hydrogen losses by hydrogenotrophic methanogenesis and hydrogen diffusion from the cathode chamber to the anode chamber [19,20].

By observing OE, all the MEDC systems in these tests were achieved much lower OE values (less than 35%) compared with previous studies [5,21]. This is because the MEDC systems suffer from severe cathodic overpotential.

3.4. Salt removal

To evaluate the desalination performance of each MEDC, the all MEDC reactors were operated over two batch cycles with no replacement of NaCl solutions in the desalination chamber. Fig. 5 describes the desalination rates and salt removal efficiencies, calculated based on the measurement of TDS, in the conventional MEDC and MEDCs with a direct proton transfer pathway. The desalination rate for a conventional MEDC (9.17 mg/L_{TDS}/L_V·h) was higher than that of MEDCs with a direct proton transfer pathway, while the salt removal efficiency for the conventional MEDC (49.70%) was lower than that for the MEDCs with a direct proton pathway. In MEDC system, the salt removal, which is the transfer of ionic species from the desalination chamber to both the anode chamber (in the case of anions) and the cathode chamber (in the case of cations), is mainly controlled by transfer of electrons, generated by bio-catalytic oxidation of substrate, from the anode to the cathode [11,22]. A previous study showed that there was a good correspondence between electrons harvested and

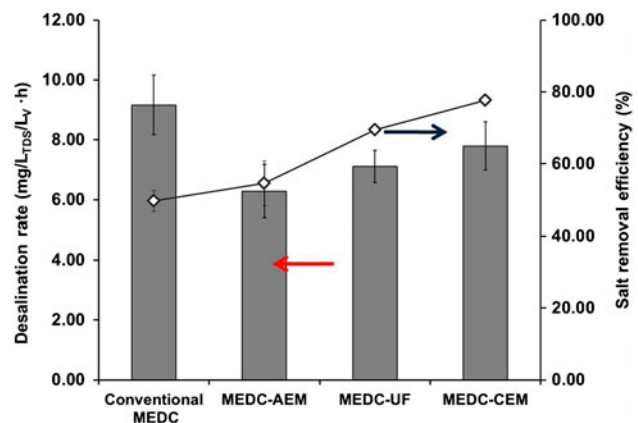


Fig. 5. The desalination rates and efficiencies of the conventional MEDC and MEDCs with a direct proton transfer pathway constructed with three different types of membranes over complete two batch cycles.

salt removal [23]. As the previous study shown, the transfer of electrons would fully contribute to the salt removal in the conventional MEDC. However, in the MEDCs with a direct proton transfer pathway, transfer of ionic species from the desalination chamber to both the anode and cathode chambers as well as a direct exchange of ionic species between the anode and cathode chambers competitively occur during the transport of electrons from the anode chamber to the cathode chamber through the external circuit; thus, the desalination rates of the MEDCs with a direct proton transfer pathway are lower than that of the conventional MEDC. However, the reason why the lowest salt removal efficiency in the conventional MEDC is due to the larger volume of the middle chamber—which means that 40 mL of NaCl solution was used in the a conventional MEDC, whereas 20 mL of NaCl solution was used in MEDCs with a direct proton transfer pathway.

In the MEDC tests with different membranes for a direct proton transfer pathway, the MEDC–CEM showed the highest desalination rate and salt removal efficiency (6.28 mg/L_{TDS}/L_V h, 77.63%), followed by MEDC–UF (7.12 mg/L_{TDS}/L_V h, 69.47%), and MEDC–AEM (7.79 mg/L_{TDS}/L_V h, 56.40%). The tendency of desalination performance with different membranes for a direct proton transfer pathway is similar with the result of pH variation in MEDCs with a direct proton transfer pathway constructed with different membranes. It can be said that higher desalination performance was observed in a MEDC, which recorded higher pH variations, with a direct proton transfer pathway. However, the ion transport in the MEDC systems with a direct proton transfer pathway is more complicated than the conventional MEDC. Thus, further study is needed to understand the salt removal from the desalination chamber in the MEDC system with the direct proton transfer pathway.

4. Conclusions

To improve the performance of MEDCs by reducing the imbalance of pH between the anode and cathode chambers, a direct proton transfer pathway was installed using three different types of membranes. Then, the effect of a direct proton transfer pathway constructed with different types of membrane on pH variations, hydrogen production, and desalination performance was investigated. The set-up of a direct proton transfer pathway can reduce the imbalance of pH between the anode and cathode chamber by up to 54%. Also, the MEDCs with a direct proton transfer pathway resulted relatively higher

hydrogen production and salt removal efficiency compared with the conventional MEDC.

In the comparison of the MEDCs with a direct proton transfer pathway constructed with different membranes, even though the MEDC–AEM showed the best ability to alleviate pH gradients, but the lower hydrogen production was observed in the MEDC–UF; this may be due to the high substrate permeability of AEM. In addition, the MEDC having higher pH variations showed higher desalination performance. The desalination performance can be related to the mass transport in MEDC system; however, the mass transport in the MEDC system with a direct proton transfer pathway was not observed in this study. Thus, it remains further research step.

Acknowledgements

This research was supported by a grant (07SeaHeroA01-01) from Plant Technology Advancement Program funded by Ministry of Land, Transport and Maritime Affairs.

References

- [1] M. Dresselhaus, I. Thomas, *Alternative energy technologies*, *Natural Gas* 21 (2001) 19–29.
- [2] D. Sperling, J.S. Cannon, *The hydrogen energy transition: Moving toward the post petroleum age in transportation*, Elsevier, Boston, MA, 2004.
- [3] D. Das, T.N. Veziroglu, *Hydrogen production by biological processes: A survey of literature*, *Int. J. Hydrogen Energy* 26 (2001) 13–28.
- [4] D.B. Levin, L. Pitt, M. Love, *Biohydrogen production: Prospects and limitations to practical application*, *Int. J. Hydrogen Energy* 29 (2004) 173–185.
- [5] B.E. Logan, D. Call, S. Cheng, H.V.M. Hamelers, T.H.J.A. Sleutels, A.W. Jeremiasse, R.A. Rozendal, *Microbial electrolysis cells for high yield hydrogen gas production from organic matter*, *Environ. Sci. Technol.* 42 (2008) 8630–8640.
- [6] D. Das, N. Khanna, N.T. Veziroglu, *Recent developments in biological hydrogen production processes*, *Chem. Ind. Chem. Eng. Q. CICEQ* 14 (2008) 57–67.
- [7] F.F. Ajayi, K.Y. Kim, K.J. Chae, M.J. Choi, I.S. Chang, I.S. Kim, *Optimization studies of bio-hydrogen production in a coupled microbial electrolysis–dye sensitized solar cell system*, *Photochem. Photobiol. Sci.* 9 (2010) 349–356.
- [8] H. Luo, P.E. Jenkins, Z. Ren, *Concurrent desalination and hydrogen generation using microbial electrolysis and desalination cells*, *Environ. Sci. Technol.* 45 (2011) 340–344.
- [9] A.D. Khawaji, I.K. Kutubkhanah, J.-M. Wie, *Advances in seawater desalination technologies*, *Desalination* 221 (2008) 47–69.
- [10] Y. Leng, G. Chen, A.J. Mendoza, T.B. Tighe, M.A. Hickner, C.-Y. Wang, *Solid-state water electrolysis with an alkaline membrane*, *J. Am. Chem. Soc.* 134 (2012) 9054–9057.
- [11] M. Mehanna, P.D. Kiely, D.F. Call, B.E. Logan, *Microbial electrodialysis cell for simultaneous water desalination and hydrogen gas production*, *Environ. Sci. Technol.* 44 (2010) 9578–9583.
- [12] K.J. Chae, M. Choi, F.F. Ajayi, W. Park, I.S. Chang, I.S. Kim, *Mass transport through a proton exchange membrane (Nafion) in microbial fuel cells*, *Energy Fuels* 22 (2007) 169–176.

- [13] S. Chen, G. Liu, R. Zhang, B. Qin, Y. Luo, Development of the microbial electrolysis desalination and chemical-production cell for desalination as well as acid and alkali productions, *Environ. Sci. Technol.* 46 (2012) 2467–2472.
- [14] R.A. Rozendal, H.V.M. Hamelers, C.J.N. Buisman, Effects of membrane cation transport on pH and microbial fuel cell performance, *Environ. Sci. Technol.* 40 (2006) 5206–5211.
- [15] Y. Zuo, S. Cheng, B.E. Logan, Ion exchange membrane cathodes for scalable microbial fuel cells, *Environ. Sci. Technol.* 42 (2008) 6967–6972.
- [16] Y. Zuo, S. Cheng, D. Call, B.E. Logan, Tubular membrane cathodes for scalable power generation in microbial fuel cells, *Environ. Sci. Technol.* 41 (2007) 3347–3353.
- [17] J.R. Kim, S. Cheng, S.-E. Oh, B.E. Logan, Power generation using different cation, anion, and ultrafiltration membranes in microbial fuel cells, *Environ. Sci. Technol.* 41 (2007) 1004–1009.
- [18] X. Zhang, S. Cheng, X. Huang, B.E. Logan, Improved performance of single-chamber microbial fuel cells through control of membrane deformation, *Biosens. Bioelectron.* 25 (2010) 1825–1828.
- [19] K.-J. Chae, M.-J. Choi, K.-Y. Kim, F.F. Ajayi, I.-S. Chang, I.S. Kim, Selective inhibition of methanogens for the improvement of biohydrogen production in microbial electrolysis cells, *Int. J. Hydrogen Energy* 35 (2010) 13379–13386.
- [20] R.A. Rozendal, H.V.M. Hamelers, R.J. Molenkamp, C.J.N. Buisman, Performance of single chamber biocatalyzed electrolysis with different types of ion exchange membranes, *Water Res.* 41 (2007) 1984–1994.
- [21] D. Call, B.E. Logan, Hydrogen production in a single chamber microbial electrolysis cell lacking a membrane, *Environ. Sci. Technol.* 42 (2008) 3401–3406.
- [22] K.S. Jacobson, D.M. Drew, Z. He, Use of a liter-scale microbial desalination cell as a platform to study bioelectrochemical desalination with salt solution or artificial seawater, *Environ. Sci. Technol.* 45 (2011) 4652–4657.
- [23] X. Cao, X. Huang, P. Liang, K. Xiao, Y. Zhou, X. Zhang, B. E. Logan, A new method for water desalination using microbial desalination cells, *Environ. Sci. Technol.* 43 (2009) 7148–7152.